Submitted, accepted and published by:

Fuel (2014) Vol. 126, pp. 239-249.

On the use of a highly reactive iron ore in Chemical Looping Combustion of different coals

T. Mendiara*, L. F. de Diego, F. García-Labiano, P. Gayán, A. Abad, J. Adánez

Department of Energy and Environment, Instituto de Carboquímica-ICB-CSIC

Miguel Luesma Castán 4, 50018, Zaragoza, Spain

tmendiara@icb.csic.es

* Corresponding author:

Phone: + 34 976 733 977;

Fax: +34 976 733 318

Abstract

Coal combustion using the Chemical Looping technology can be carried out under different configurations. This paper focuses on the *in situ* gasification Chemical Looping Combustion (*i*G-CLC). In this technology, it is especially important the selection of the oxygen carrier as there may be losses in the drainage of coal ashes. Finding low-cost oxygen carriers has become a relevant research focus. Several Fe-based materials have been tested including minerals and industrial residues. In this work, a highly reactive iron ore that had already shown promising characteristics for coal combustion was used in a continuous 500 W_{th} CLC unit. Its performance in the combustion of anthracite, bituminous coal and lignite was evaluated and compared with the results for other Fe-based materials, such as ilmenite or bauxite waste. The combustion efficiency obtained with the Tierga iron ore was the highest reported to date which makes this carrier a promising candidate for further scale-up. Moreover, the high CaO content of this material led to analyze its relevance for sulphur removal during the first hours of operation. High sulphur retention capacity was observed but this capacity decreased with time as the calcium oxide was both saturated and lost as fines during operation.

Keywords: combustion, coal, CO_2 capture, chemical looping, iron ore

1. Introduction

According to IEA statistics, carbon dioxide emissions from fossil fuel combustion for heat and power production accounted for 41% of world CO_2 emitted in 2008 [1]. The principal fuel used in this sector is coal, the most carbon-intensive of fossil fuels and its use is expected to become even more widespread in certain world regions. In order to mitigate the impact of CO_2 emissions on climate change, CO_2 Capture and Storage (CCS) emerged as an option to reduce CO_2 emissions from the power sector by separating CO_2 from the rest of combustion gases and storing it in a safe place. Thus CO_2 emission to the atmosphere is avoided. Among the different CO_2 capture technologies already investigated, this paper focuses on Chemical Looping Combustion (CLC). In this technology, the combustion of the fossil fuel takes place avoiding the direct contact between fuel and air. The presence of an oxygen carrier, normally a metal oxide, allows for the transfer of oxygen from air to fuel possible by means of a redox reaction. The oxygen carrier circulates between two reactors, called fuel and air reactors. The oxygen carrier is reduced in the fuel reactor and the oxygen transferred in this process oxidizes the fuel to CO_2 and H_2O. The reduced oxygen carrier is then conveyed to the air reactor, where it is oxidized back to the initial state. Then, the oxygen carrier is sent again to the fuel reactor to start a new redox cycle allowing the continuous combustion of the fuel.

Different configurations have been described for CLC of coal, but most of them consider interconnected fluidized beds for fuel and air reactors. This paper is based on the *in situ* Gasification Chemical Looping Combustion (*i*G-CLC) [2]. According to the *i*G-CLC scheme, coal is introduced directly to the fuel reactor where it is gasified. Steam or CO_2 or even mixtures of both are commonly used as gasifying agents. The following equations summarize the processes taking place:

$$\text{Coal} \rightarrow \text{Volatiles} + \text{Char (C)} \quad (1)$$

$$\text{Char (C)} + H_2O \rightarrow H_2 + CO \quad (2)$$

$$\text{Char (C)} + CO_2 \rightarrow 2\ CO \quad (3)$$

$$H_2 + M_xO_y \rightarrow H_2O + M_xO_{y-1} \quad (4)$$

$$CO + M_xO_y \rightarrow CO_2 + M_xO_{y-1} \quad (5)$$

$$CH_4 + 4\ M_xO_y \rightarrow CO_2 + 2\ H_2O + 4\ M_xO_{y-1} \quad (6)$$

The reduced oxygen carrier is then transferred to the air reactor where it is re-oxidized again:

$$M_xO_{y-1} + ½\ O_2 \rightarrow M_xO_y \quad (7)$$

The performance of the CLC technology can be evaluated by the carbon capture and combustion efficiency of the process. High values of carbon capture efficiency indicate that most of the carbon in the coal fed can be found in the gaseous stream at outlet of the fuel reactor and therefore captured. In order to maintain high carbon capture values, the transfer of carbon from fuel to air reactor should be minimized as the carbon dioxide emitted in the air reactor is not captured. Therefore, the residence time of char in the fuel reactor should be long enough for the char to be gasified [3-5]. To improve char conversion maintaining a reasonable reactor size, the use of a carbon separation unit was proposed [6], where unconverted char is separated from oxygen carrier particles and sent back to the fuel reactor.

High combustion efficiency values are related to the absence of unburned compounds at the outlet of the fuel reactor. The combustion efficiency in *i*G-CLC is evaluated using the oxygen demand, which indicates the fraction of oxygen demanded by unconverted compounds exiting from the fuel reactor (CH_4, H_2 or CO) with respect to the oxygen required to burn the solid fuel. The oxygen demand would be directly related to the O_2 requirements in a hypothetical oxygen polishing step downstream the fuel reactor [7]. The presence of

unconverted compounds in *i*G-CLC has been reported before in units ranging 0.5-100 kW_{th} with different oxygen carriers and solid fuels [8-17] and represents both energy and CO_2 quality losses [18]. Recent investigations try to decrease the oxygen demand of the process, which includes optimization of operational conditions, design modifications or use of highly reactive materials [18-21]. Recently, a summary of experimental data obtained in different experimental units under different combustion conditions was presented by Gayán et al. [19]. The analysis of the data allowed them to evaluate the impact of the type of solid fuel, the oxygen carrier material and the solids inventory on the oxygen demand. The majority of the results that were considered used ilmenite as oxygen carrier. Ilmenite is a mineral found in methamorphic and igneous rocks. The principal constituent of ilmenite is $FeTiO_3$. The oxygen demand values reported for ilmenite under different experimental conditions varied between 5-15%. Experimental results obtained in different CLC units with different oxygen carriers and different coals suggest that the use of oxygen carriers with higher reactivity than ilmenite (based on Ni or Fe) allowed reaching lower values of oxygen demand for the same solids inventory in the fuel reactor. Also, it was found that solid fuels with an important volatile content usually showed higher oxygen demand values. Theoretical calculations confirmed that the oxygen carrier reactivity notably influenced the oxygen demand [19-20].

On the other hand, being cost-competitive and easy to dispose are two features that become especially significant in an *i*G-CLC system burning coal. Depending on the ash content of the coal, it could be necessary to periodically drain the coal ashes from the CLC system. Otherwise, they would accumulate and generate operational problems. Therefore some oxygen carrier particles can be lost together with the ashes during this process and that is the reason to look for cheap and environmentally friendly materials. According to this, Fe-based materials represent a more interesting option for *i*G-CLC of coal. Although they are not as

125 reactive as metal oxides like NiO, they present the advantage of their low cost and non-toxic
126 nature [2]. In many recent studies the oxygen carriers tested in *i*G-CLC units with coal were
127 industrial residues and minerals [17,22-23].
128
129 In the research group at Instituto Carboquimica ICB-CSIC different Fe-based materials have
130 been tested as oxygen carriers for *i*G-CLC. Those tests included chemical and physical
131 characterization of ilmenite, a bauxite waste generated in the alumina production through the
132 Bayer process (Fe-ESF), an iron ore from a hematite mine in Tierga (Zaragoza, Spain) and a
133 copper ferrite ore [24,25]. The Tierga iron ore and Fe-ESF showed promising characteristics
134 compared to the other materials tested. Compared to ilmenite, a significant reduction of the
135 oxygen demand was attained with the use of Fe-ESF in a continuous unit [22]. Based on
136 previous results [24], the use of this Tierga iron ore for *i*G-CLC processes with coal could
137 represent a significant improvement in the combustion efficiency and reduce the solids
138 inventory needed without a high investment due to the high cost associated to reactive
139 materials, as this material is available at low cost. The reactivity of this iron ore was similar
140 to that of a synthetic Fe_2O_3-based oxygen carrier and even higher in the case of the reaction
141 with hydrogen. The mechanical properties were also good, with high values of mechanical
142 strength which were maintained through the successive redox cycles [24].
143
144 The aim of this work is to evaluate the highly reactive Tierga iron ore in relation to the
145 combustion efficiency and carbon capture which could be reached using this material as
146 oxygen carrier. Due to its CaO content, the Tierga iron ore could also be capable of retaining
147 the sulphur compounds generated during coal combustion. This possibility will be also
148 evaluated. Experimental work was performed in a continuous CLC unit using different types

149 of coal and results were compared with those previously obtained using ilmenite and Fe-ESF
150 under similar conditions.
151
152 **2. Experimental**
153 **2.1 Materials used**
154 The iron ore used as oxygen carrier in this work was provided by PROMINDSA from a
155 hematite mine in Tierga (Zaragoza, Spain). The procedure to characterize this material has
156 been described in detail elsewhere [24]. Once received, the iron ore was first crushed and
157 sieved to the desired size (+100-300 μm). XRD diffraction identified as main solid phases
158 hematite (Fe_2O_3), dolomite ($CaMg(CO_3)_2$) and SiO_2. Prior to be used, the iron ore was
159 calcined at 950ºC during 12 hours, so that the dolomite in the sample decomposes to CaO and
160 MgO. The calcination of the material also increased the mechanical strength of the iron ore.
161 Table 1 shows the main chemical and physical properties of the calcined material.
162
163 Spanish anthracite from "El Bierzo", bituminous Colombian coal "El Cerrejón" and Spanish
164 lignite were used as fuel in the experiments. Table 2 shows the proximate and ultimate
165 analyses of the coals together with the lower heating value. All of them were milled and
166 sieved (+200-300 μm for lignite and Colombian coal and +75-300 μm for anthracite). The
167 bituminous coal was subjected to a thermal pre-treatment for pre-oxidation (180ºC in air for
168 28 hours) to avoid agglomeration of the fluidized bed due to its strong swelling tendency [9].
169
170 **2.2 Experimental setup and procedure**
171 All the experiments were performed in a continuous unit (ICB-CSIC-s1). This experimental
172 setup is shown in Figure 1 and consists of two fluidized bed reactors, fuel (1) and air (3)
173 reactors, connected by another fluidized bed acting as loop seal (2). The fuel reactor is a

bubbling fluidized bed (50 mm ID and 200 mm bed height) where the coal (9) is fed at the bottom and just above the fuel reactor distributor plate. Steam is fed to the fuel reactor as fluidizing gas and also as the coal gasifying medium. The oxygen carrier is reduced in the fuel reactor bed by reaction with the gases generated during coal devolatilization/gasification and sent to the air reactor. The reduced oxygen carrier is re-oxidized in the air reactor (80 mm ID and 100 mm bed height). Secondary air was introduced above the bubbling bed to help entrainment along the riser (4). A high-efficiency cyclone (5) recovered the particles in a solid reservoir (7) which avoids mixing atmospheres between the fuel reactor and the riser. The solid flow returning to the fuel reactor was regulated by a solid valve (8) and the value of this flow could also be measured with a diverting solid valve (6).

At the beginning of the experimental runs, 3.3 kg of Tierga iron ore were introduced into the CLC unit. The solids in the fuel reactor were around 0.6 kg. The steam flow to the fuel reactor was 200 L_N/h, corresponding to a velocity of 0.14 m/s at 900ºC. Coal was fed at 85 g/h. The oxygen carrier to fuel ratio (ϕ) is commonly used to compare the oxygen supplied by the circulating oxygen carrier to the oxygen needed to burn the fuel:

$$\phi = \frac{\dot{m}_{OC} \cdot R_{OC}}{\Omega_{SF}} \tag{8}$$

Stoichiometric conditions correspond to values of ϕ equal to 1. These conditions were maintained throughout the tests by adjusting the value of the oxygen carrier circulation rate. In the air reactor the total primary air flow was 1800 L_N/h (corresponding to a velocity of 0.45 m/s at 900ºC). The secondary air flow was 480 L_N/h. The sum of the primary and secondary air flow gives a gas velocity in the riser around 2 m/s. The nitrogen flow in the loop seal was 90 L_N/h.

Lignite, anthracite and bituminous Colombian coal were used as fuels in the continuous unit with the Tierga iron ore. In these experiments, the fuel reactor temperature was changed between 875 to 930ºC. In the air reactor, the temperature was set to 950ºC. In total, the Tierga iron ore experienced around 50 hours of continuous hot fluidization and 30 hours of coal combustion. Solid samples from both fuel and air reactors have been extracted from the unit in order to analyze their composition and the effect of the time of operation on the properties of the oxygen carrier. Sampling bags were used to analyze the presence of C_2-C_4 hydrocarbons in the outlet stream from the fuel reactor. Tar measurements were also conducted using the tar protocol [26].

The values of CO, CO_2, and CH_4 concentration at outlet of the fuel reactor were measured using nondispersive infrared (NDIR) analysers while a paramagnetic analyzer determined O_2 concentration and a thermal conductivity detector was used for H_2. The H_2S and SO_2 concentration at the outlet of the fuel reactor was monitored and registered in order to determine the fate of the sulphur liberated in coal combustion. SO_2 concentration was determined using an infrared Siemens Ultramat 23 analyzer. For the determination of H_2S, gas chromatograph (Varian 3400-CX GC) with a PORAPAK-Q packed column for chromatographic separation and a sulphur-specific flame photometric detector (FPD) was used. All data were collected by means of a data logger connected to a computer.

2.3. Data evaluation

The carbon capture efficiency (η_{CC}) has commonly been defined as the fraction of the carbon introduced converted to gas in the fuel reactor. The carbon converted is calculated from the CH_4, CO and CO_2 exiting the fuel reactor, as the amount of tars and hydrocarbons heavier than CH_4 was negligible.

$$\eta_{CC} = \frac{[F_{CO_2,FR} + F_{CO,FR} + F_{CH_4,FR}]_{out}}{[F_{CO_2,FR} + F_{CO,FR} + F_{CH_4,FR} + F_{CO_2,AR}]_{out}} \quad (9)$$

The carbon captured in the system is the carbon contained in the volatiles and the carbon in the char that is gasified. Thus, the carbon capture efficiency calculated according equation (9) depends on the fraction of char that has been gasified. The char conversion (X_{char}) is defined as the fraction of carbon in the char formed in the fuel reactor which is released to the fuel reactor exhaust gas stream:

$$X_{char} = \frac{[F_{CO_2,FR} + F_{CO,FR} + F_{CH_4,FR} - F_{C,vol}]_{out}}{[F_{CO_2,FR} + F_{CO,FR} + F_{CH_4,FR} + F_{CO_2,AR} - F_{C,vol}]_{out}} \quad (10)$$

The gasified char in the fuel reactor was calculated as the difference between the carbon in the outlet gases of the fuel reactor and the carbon flow coming from the volatile matter, $F_{C,vol}$. The carbon content in the volatiles is calculated using the ultimate and proximate analysis of the coal as the difference between the total carbon in coal and the fixed carbon. Nevertheless, carbon losses as elutriated char particles at the outlet of the fuel reactor have been reported in different experimental units [19]. The fraction of carbon in the coal which is elutriated is calculated from the carbon mass balances to the system considering the difference between the carbon in the coal fed and the carbon measured in the gaseous stream at the outlet of the fuel reactor. The losses due to carbon elutriation may affect the value of carbon capture defined in equation (9), especially if the fraction of carbon elutriated is high. To overcome discrepancies on carbon capture efficiency due to the char elutriation, the use of an estimated carbon capture efficiency is here proposed, η_{CC}^{*}. This parameter represents the expected carbon capture in the iG-CLC unit if no char was elutriated from the fuel reactor and assumes

that the char conversion would be the same in this case, as temperature is the most influencing variable affecting char gasification rate [27]. Thus, the value of the carbon capture can be estimated using the ultimate and proximate analysis of the coal and the char conversion obtained in the CLC unit, see equation (11). The value of X_{char} is calculated using equation (10).

$$\eta_{CC}^{*} = 1 - \frac{C_{fixed}}{C_{coal}} \cdot (1 - X_{char}) \tag{11}$$

The total oxygen demand (Ω_T) is defined as the fraction of stoichiometric oxygen required to fully oxidize the unconverted gases exiting the fuel reactor to CO_2 and H_2O with respect to the stoichiometric oxygen demand of the coal fed.

$$\Omega_T = \frac{0.5 \cdot F_{CO,FR} + 2 \cdot F_{CH_4,FR} + 0.5 \cdot F_{H_2,FR}}{(\dot{m}_{SF} \cdot \Omega_{SF} / M_{O_2})} \tag{12}$$

The oxygen demand is linked to the reactivity of the oxygen carrier. This reactivity can be evaluated by the rate of oxygen transferred by the oxygen carrier in the CLC unit, ($-r_O$). This rate is calculated as the oxygen gained in the oxygen-containing gases (CO, CO_2 and H_2O) divided by the amount of oxygen carrier in the fuel reactor ($m_{OC,FR}$):

$$(-r_O) = M_O \frac{[F_{H_2O,FR} + 2 \cdot F_{CO_2,FR} + F_{CO,FR}]_{out} - [F_{H_2O,FR}]_{in}}{m_{OC,FR}} \tag{13}$$

3. Results and Discussion

3.1 Testing with different coals

Experiments with different types of coal such as lignite (L), bituminous with high volatile content (HVB) and anthracite (A) were performed in order to evaluate the potential of the Tierga iron ore as oxygen carrier. In all the experiments presented, stoichiometric conditions were maintained and different temperatures in the fuel reactor were tested in the range 875-930ºC. In all the cases, steam was used as gasifying agent. Figure 2 summarizes the main results obtained showing the total oxygen demand and the carbon capture efficiency as representative parameters of the performance of the process. It is remarkable that in all the cases in Figure 2 (A) the total oxygen demand was always below 4%. The lowest values were obtained in experiments with the bituminous Colombian coal (HVB) and lignite. Using these coals as fuels, the oxygen demand reached values lower than 2% at 920ºC. This result confirms that the Tierga iron ore is able to convert gasification products and volatile matter to CO_2 and H_2O to a large extent. Note that volatiles are the major contribution to unburned compounds in this unit, whose fuel reactor is in the bubbling regime [9]. However the oxygen demand in the experiments with anthracite was higher, although the volatile content in this coal was the lowest. This fact was attributed to the size of the anthracite particles (+75-300 μm), considerably lower than that employed in the experiments with both lignite and Colombian coal (+200-300 μm). It has been already observed that the size of coal particles affect the oxygen demand. If the size of coal particles is low, the coal particles can leave the fuel reactor swept along the gaseous stream. These unconverted particles can be gasified in the freeboard of the fuel reactor due to the excess of steam present, yielding CO an H_2. These gases can not react with the oxygen carrier particles and therefore, contribute to the increase in the oxygen demand [28].

Figure 2 (B) shows the values of carbon capture efficiency obtained for the experiments with different coals. Closed symbols represent the experimental values and open symbols represent the estimated carbon capture when no elutriation occurred. Differences were observed between the experimental values for carbon capture and those estimated in the absence of elutriation. The largest differences corresponded to the bituminous Colombian coal (up to 6 percentage points), although in the case of anthracite the elutriation was the highest due to the lower size of the anthracite particles. The differences between the experimental values and those estimated without elutriation are mainly attributed to the differences both in the fixed carbon content of the different coals and char conversion reached in each case. For the different coals tested, the values of carbon capture efficiency increased following the sequence: anthracite < bituminous Colombian (HVB) < lignite. The low carbon capture values obtained for the bituminous and anthracite coal were due to the low reactivity of these coals. This fact suggests the need of a carbon separation unit to increase the residence time of char particles in the fuel reactor, and hence the carbon capture. However, high carbon captures (94% at 920ºC) were reached with lignite with a solids inventory in the fuel reactor of 2023 kg/MW_{th}. This solids inventory can be assumed for an *i*G-CLC system and the presence of a carbon separation unit could not be required in this case.

3.2 Comparison with other low-cost Fe-based materials

The main objective of the present work was to investigate the improvements on combustion that the use of the Tierga iron ore as oxygen carrier can bring to the *i*G-CLC process. This necessarily includes a comparison with other oxygen carriers recently proposed in literature. Among the Fe-based low-cost materials tested in continuous units, there are two that received especial attention, namely ilmenite and a Fe-enriched sand fraction from alumina production (Fe-ESF). Both the Fe-ESF material and ilmenite have been tested by the authors in this same

316 experimental unit [22]. Therefore, the results obtained with the Tierga iron ore will be
317 compared to those obtained using ilmenite and Fe-ESF in the same CLC rig and for the same
318 bituminous Colombian coal (HVB) [9,22]. The comparison will be based on the analysis of
319 both the total oxygen demand and the carbon capture efficiency obtained under different
320 temperatures in the fuel reactor. Stoichiometric conditions were considered in all the
321 experiments ($\phi = 1$). The values of total oxygen demand at different fuel reactor temperatures
322 for ilmenite, Fe-ESF and the Tierga iron ore (Fe-ore) are presented in Figure 3 (A). The
323 experiments were performed with a solids inventory in the fuel reactor of 3140 kg/MW_{th} in
324 the case of ilmenite, 2850 kg/MW_{th} for the Fe-ESF material and 1463 kg/MW_{th} for the Tierga
325 iron ore. The total oxygen demand decreases with temperature for all oxygen carriers.
326 However, lower values of oxygen demand were obtained using the Tierga iron ore regardless
327 of the temperature, although a lower amount of solids per thermal power was used. In this
328 case the oxygen demand was always lower than 3%. This could be explained by the higher
329 reactivity of the Tierga iron ore to the main gases present in the fuel reactor (CO, H_2, CH_4),
330 especially when compared to ilmenite [24]. In order to further compare the reactivity of this
331 three oxygen carriers the rate of oxygen transfer ($-r_O$) was calculated and shown in Figure 3
332 (B). The rate of oxygen transferred from the oxygen carrier to the fuel increases as
333 temperature increases. At 930ºC the value of ($-r_O$) for Fe-ESF is $2.1 \cdot 10^{-5}$ kg O_2/s·kg oxygen
334 carrier, around 1.5 times that obtained for ilmenite. At 920ºC, a slightly lower temperature,
335 the rate of oxygen transferred from the Tierga iron ore was $3.4 \cdot 10^{-5}$ kg O_2/s·kg oxygen
336 carrier, higher than the observed for the other two carriers although it was obtained with
337 lower solids inventory. The faster oxygen transfer rates of the Tierga iron ore represent an
338 important advantage compared to the other Fe-based materials and would significantly
339 contribute to reduce the needs in the oxygen polishing step.

Another paramenter to be considered is the carbon capture efficiency. The experimental values for the different materials in the experiments with the bituminous Colombian coal are shown in Figure 4 (A). The values increased with temperature for the three oxygen carriers as char gasification is more favored at higher temperatures. There are not relevant differences between the values obtained for the three oxygen carriers. All of them oscillate between 42 and 71%. According to equation (11), this indicates that the char conversion values obtained in these experiments with the different materials should be similar. The conversion values were calculated and resulted similar for ilmenite, the Fe-ESF and the Tierga iron ore. Nevertheless, considering the solids inventory and solid circulation rate in the experiments the residence time in the fuel reactor should be different for the three materials. The residence time assuming no elutriation was calculated as:

$$t_{res} = \frac{m_{OC,FR}}{F_{OC}} \tag{14}$$

The residence times for the Tierga iron ore, Fe-ESF and ilmenite ore resulted 7, 12 and 24 minutes, respectively. Therefore, the Tierga iron ore particles allowed to reach similar char conversion values to those obtained with ilmenite although the time for the char to be converted was three times lower. In order to investigate this result, the char gasification rate of the bituminous Colombian coal in the experiments with the three oxygen carriers was calculated.

$$(-r_C) = \frac{X_{char}}{t_{res} \cdot (1 - X_{char})} \tag{15}$$

The char gasification rates obtained for this coal were plotted in Figure 4 (B). As expected, the gasification was favored at the highest temperatures and higher gasification rates were observed. Nevertheless, the gasification of the char was around four times faster in the experiments with the Tierga iron ore compared to ilmenite. The previously highlighted differences in the reactivity of both materials can explain this behavior. The Tierga iron ore reacts faster than ilmenite with the CO and H_2 generated during char gasification. The decrease in the concentration of these gases reduces their inhibition effect on char gasification, thus the gasification proceeds faster [29]. It can be considered that the gasification of the char can be described by the homogeneous reaction model with chemical reaction control:

$$(-r_C) = \frac{k_{react} \cdot p_{react}}{1 + \cdot K_{react} \cdot p_{react} + K_{prod} \cdot p_{prod}} \quad (16)$$

where p_{react} is the partial pressure of the gaseous reactants (H_2O in this case), p_{prod} is the partial pressure of the gasification products (CO and H_2) and k_{react} is the kinetic constant. K_i considers the inhibitory effect of products and reactants in gasification. Values for this bituminous Colombian coal were determined in a previous work [30]. The gasification rate for the bituminous Colombian coal was calculated according to equation (16) using the values of p_{react} and p_{prod} measured at 920ºC with the three Fe-based materials at the outlet of the fuel reactor. The comparison with the experimental values in Figure 4(A) is presented in Figure 5 as a function of the sum of CO and H_2 concentrations in the outlet stream. The highest concentration of these gases was observed for ilmenite followed by the Fe-ESF material and the Tierga iron ore. The higher the concentration of these gases the lower the

385 char gasification rate. This experimental trend was captured by the kinetic expression in
386 equation (16). According to Figure 5 good agreement between experimental and theoretical
387 values was observed. Therefore, the Tierga iron ore minimizes the inhibition effect of CO and
388 H_2 on gasification and the gasification proceeds faster. Thus, similar char conversion to
389 ilmenite can be attained with shorter residence time and therefore, lower solids inventory.
390 This represents a significant advance in the scale-up of the process, as lower solids
391 inventories allow smaller reactor sizes.

392

393 In a real CLC system, the carbon capture efficiency will be enhanced by the presence of a
394 carbon separation unit [6]. In this unit, the unconverted char particles leaving the fuel reactor
395 are separated from the oxygen carrier particles and returned back to the fuel reactor. The char
396 conversion obtained is higher compared to that in the absence of this unit and therefore,
397 higher carbon capture efficiencies are achieved. For a more realistic comparison of the carbon
398 capture efficiencies that would be obtained using each of the low-cost Fe-based materials, a
399 simple calculation was done from the experimental results based on the char gasification rate
400 ($-r_c$) obtained at the corresponding temperature and the carbon separation efficiency in the
401 carbon separation unit (η_{CSS}) [24]. The efficiency in the carbon separation unit is defined as
402 the fraction of carbon separated in this unit compared to carbon entering the unit:

403

404 $$\eta_{CC} = 1 - \frac{C_{fixed}}{C_{coal}} \cdot \frac{F_{OC} \cdot (1 - \eta_{CSS})}{(-r_C) \cdot m_{s,FR} + F_{OC} \cdot (1 - \eta_{CSS})} \quad (17)$$

405

406 Figure 6 shows the carbon capture efficiencies estimated for the three oxygen carriers at
407 920ºC for different η_{CSS} values. As it was known, the carbon capture efficiency increased

408 with the value of the efficiency in the carbon separation unit. The differences between
409 oxygen carriers are reduced with the increase in the η_{CSS} value. The carbon capture efficiency
410 was higher than 97% for all the carriers assuming η_{CSS} equal to 0.98. This efficiency of the
411 carbon separation unit was easily reached during operation in a 100 kW_{th} CLC unit [31].
412 Therefore no significant differences in the carbon capture efficiencies will be expected
413 between ilmenite, Fe-ESF and the Tierga iron ore if an efficient separation of the unconverted
414 char from the oxygen carrier particles is performed at the outlet of the fuel reactor and the
415 unconverted char is sent back to this reactor. Considering the results obtained in similar
416 conditions for ilmenite, Fe-ESF and the Tierga iron ore it can be said that the Tierga iron ore
417 is the most promising material to be considered for *i*G-CLC. The Tierga iron ore presents
418 higher reactivity to H_2 and CO than ilmenite and Fe-ESF, which results in very low values of
419 oxygen demand at the outlet of the fuel reactor with lower solids inventory. Besides, using a
420 carbon separation unit between fuel and air reactors, the carbon capture efficiency at high
421 temperatures can be significantly increased.

422

423 Other characteristics also make the Tierga iron ore a suitable material to be considered for the
424 further scale up of the *i*G-CLC process. Figure 7 shows the evolution of the attrition rate of
425 the Tierga iron ore with time. The attrition rate was calculated as the mass percentage of
426 particles with a size smaller than 40 μm lost per hour of operation. At the beginning of the
427 experimental tests, the attrition rate was high, around 0.7%/min, but after 4.5 hours of
428 continuous hot fluidization, it decreased to a value close to 0.1%/h. This attrition rate was
429 approximately maintained through the rest of the experiments using different coals and
430 corresponds to a lifetime of the oxygen carrier of 1000 h, which can be considered adequate
431 if one takes into account its very low cost. Besides, the mechanical strength of the particles

after use was significantly high (2.3 N). These characteristics of the Tierga iron ore together with its reactivity reinforce its adequacy for the use in *i*G-CLC.

These results obtained in the ICB-CSIC-s1 unit allow to screen out materials to be tested in larger scale units. It was proved that lower oxygen demand values can be obtained with the Tierga iron ore compared to other promising candidates like ilmenite and it also possesses good mechanical properties. Similar behaviour would be expected in semi-industrial scale units.

3.4 Sulphur retention capacity of the Tierga iron ore

According to the XRD analysis in Table 1, the main solid phases in the Tierga iron ore used in this work are Fe_2O_3 together with SiO_2, Al_2O_3, CaO and MgO. An ICP analysis was carried out in order to quantify the amount of each of the components. Table 3 presents the results for the composition of the Tierga iron ore. The amount of Fe_2O_3 obtained by ICP is slightly higher than that showed in Table 1. It should be reminded that the Fe_2O_3 percentage in Table 1 corresponds to the amount of iron reducible species able to take part in chemical looping processes and was determined in a TGA using 15% H_2 at 950ºC. The CaO content of the Tierga iron ore in Table 3 is especially high (4.7%). This fact could turn quite interesting for CLC regarding the quality of the CO_2 captured in the fuel reactor. Once the fuel is fed to the fuel reactor bed, the sulphur in coal is split between volatiles and char. The main sulphur species in volatiles is H_2S, which can react with oxygen carrier particles yielding SO_2. High temperatures seem to enhance the conversion of H_2S to SO_2, so that a mixture of both species can be found in the gaseous outlet stream of the fuel reactor [11]. The presence of sulphur compounds negatively affects the quality of the CO_2 as they cause corrosion problems

456 downstream. The CaO present in the Tierga iron ore could react with the H_2S and SO_2
457 formed during combustion according to the scheme:
458
459 $CaO + H_2S \rightarrow CaS + H_2O$ (18)
460 $4\ CaO + 4\ SO_2 \rightarrow CaS + 3\ CaSO_4$ (19)
461
462 Therefore, the presence of sulphur compounds at the outlet of the fuel reactor could be
463 already reduced and controlled by the oxygen carrier which would represent a significant
464 advantage. Thus, it was considered interesting to further investigate the possible sulphur
465 retention capacity of this Tierga iron ore in *i*G-CLC experiments. For this purpose, Spanish
466 lignite with high sulphur content was used as fuel during the first hours of operation after the
467 introduction of the calcined Tierga iron ore into the system. The temperature in the fuel
468 reactor during these experiments remained at 915ºC.
469
470 Figure 8 shows the evolution of the SO_2 concentration (dry basis) in the fuel reactor working
471 at 915ºC. At the beginning of the experiment, no SO_2 was measured at the outlet of the fuel
472 reactor. The absence of SO_2 was interesting as it indicates that the CaO present in the Tierga
473 iron ore was able to react with SO_2 and eliminate it from the gaseous stream. Several
474 measurements were performed afterwards. These measurements showed that the SO_2
475 concentration increased with time quite fast during the first 2.5 hours of operation. After that
476 moment, the SO_2 concentration continued to increase, although at slower rate and at the end
477 of the experimental test, there was a trend to become stable at around 15000 ppm (dry basis).
478 The capacity of the Tierga iron ore to retain sulphur decreases quite fast and can be
479 considered lost after 4-5 hours. Considering the coal feeding rate (85 g/h) and the sulphur
480 content in the lignite showed in Table 2, the molar flow of sulphur fed was estimated as 0.14

481 mol/h. On the other hand, the amount of CaO in the system can be estimated as 2.77 mol Ca.
482 According to equations (18) and (19), the molar ratio for the reaction between CaO and
483 sulphur species is Ca/S=1. Using these values, the time expected for complete conversion to
484 CaS or $CaSO_4$ of the CaO in the Tierga iron ore would be 20 hours. This would correspond to
485 an effective CaO concentration in the iron ore circulating in the system 8 times lower, i.e.
486 around 0.6% CaO. There would be several reasons for this fast decrease in the sulphur
487 retention capacity of the Tierga iron ore. There could be a low use of the CaO present in the
488 Tierga iron ore or maybe the CaO was lost during the combustion process.
489
490 In order to further investigate the reasons for this fast decrease, several samples, labelled A, B
491 and C in Figure 8 were taken from the fuel reactor bed at different times (0.5, 2 and 5 hours,
492 respectively). X-Ray diffractograms corresponding to these samples were obtained and
493 compared to the calcined Tierga iron ore. The crystalline species initially identified in the
494 Tierga iron ore were Fe_2O_3, SiO_2, Al_2O_3, CaO and MgO. In both samples A and B, the major
495 species were SiO_2, Fe_2O_3 and Fe_3O_4. However, in sample C, the presence of $CaSO_4$ was
496 detected. It seems that after 5 hours the CaO in the oxygen carrier had been converted to
497 $CaSO_4$ in a significant extent and is not able to react with SO_2 any more. These fresh and
498 used particles were also observed using a Scanning-Electron-Microscope (SEM) equipped
499 with an EDX analyzer. Figure 9 shows the Fe, Ca and Mg profiles in fresh and used particles.
500 In the fresh particle it can be observed that after calcination Ca and Mg concentrate in the
501 external surface of the iron ore particles. The core of the particle is mainly constituted by Fe.
502 After operation in the continuous unit, it can be observed that the external surface of the
503 Tierga iron ore particles is not more Ca and Mg enriched. It seems that some Ca and Mg
504 present in particles are lost during operation. To check this loss, the fines escaping the
505 cyclone obtained during 50 hours of operation were collected and characterized. Previously

506 to the introduction of lignite, the Tierga iron ore experienced 9 hours of hot fluidization. The
507 X-Ray diffractograms of the fines collected during this time revealed the presence of SiO_2,
508 Fe_2O_3 and CaO, confirming that CaO in the oxygen carrier particles was lost in the fines,
509 maybe due to its lower mechanical strength compared to Fe_2O_3. When lignite was fed, the
510 presence of $CaSO_4$ and CaS was also observed in the fines collected.
511
512 According to the previous results, it can be concluded that the retention of sulphur
513 compounds by the Tierga iron ore is possible but decreases after a short time of operation.
514 Both the conversion of CaO in the Tierga iron ore to CaS or $CaSO_4$ and the loss of Ca and
515 Mg in the surface of the iron ore particles lead to a fast decrease in the SO_2 retention by the
516 oxygen carrier. It can be considered that the steady state in the experiments with lignite
517 showed in Figure 8 was reached after 5 hours feeding coal (sample C). Under steady state, no
518 more SO_2 retention by CaO was observed. This can be confirmed when the sulphur emissions
519 measured at the gaseous outlet from the fuel and air reactors are compared to the sulphur
520 measured using this same lignite and ilmenite as oxygen carrier [11]. Figure 10 shows the
521 sulphur distribution with respect to the total sulphur fed obtained for both ilmenite and the
522 Tierga iron ore at 910 and 915ºC, respectively. In the experiments with the Tierga iron ore,
523 once the steady state was reached, around 75 % of the sulphur fed with lignite was released in
524 the gaseous streams from both fuel and air reactors. In the fuel reactor, mainly SO_2 was
525 measured and only small amounts of H_2S were registered (H_2S/SO_2 molar ratio around 0.25).
526 In the air reactor, SO_2 was the only sulphur species found. This result was similar to what
527 was previously determined for ilmenite, therefore it can be said that the Tierga iron ore is not
528 retaining any SO_2 under these conditions. As it was explained in our previous experiments
529 with ilmenite, the rest of the sulphur fed and not measured in the experiments with the Tierga
530 iron ore can be retained by the CaO present in the ashes of this lignite (up to 15%), lost

together with the fly ashes (pyritic sulphur) (up to 4.6%) or lost in the coal elutriated during the feeding to the system [11].

If some of the SO_2 formed could be eliminated *in situ* in the fuel reactor bed the needs of the post-treatment of the fuel reactor gas in a desulphurization unit would be reduced. In order to maintain the sulphur retention capacity of the oxygen carrier in the system at a certain level, a frequent addition of fresh material would be necessary. However, the advantage of the Tierga iron ore used in this study is that it is a low-cost material, available in large quantities. This would compensate the need for a frequent replacement. Some calculations were done to determine the order of magnitude of the sulphur retention that could be achieved. The calculations considered 1 MW thermal power of lignite. As a reference, a solids inventory in the fuel reactor of 1000 kg/MW_{th} was taken into account. Then, it is estimated that the total inventory in the system considering both the solids in loop seal and air reactor would be 2000 kg. Following the results in Figure 7 the lifetime of the carrier was estimated to 1000 h. Thus, in order to maintain the solids inventory, a makeup flow of Tierga iron ore of 2 kg/h would be needed. This corresponds to the feed of $4.7 \cdot 10^{-4}$ mol/s of CaO. The sulphur introduced in 1 MW_{th} power of lignite is around 0.1 mol/s, thus the Ca/S ratio would be 0.0047, corresponding to approximately 0.5% sulphur retention, which is actually quite low. Similar calculations to those described above were performed assuming different lifetimes of the Tierga iron ore. The results are shown in Figure 11 (A) as a solid line. It can be observed that the sulphur retention increased as the lifetime decreased. Nevertheless, too much frequent replacements of the Tierga iron ore would be needed in order to achieve significative sulphur retentions. As an example, 5% sulphur retention would be obtained for a lifetime of 100 h using lignite as fuel. Considering the quick loss of CaO during the first hours of operation lower retention values could be expected. The dashed line in Figure 11 (A) represents the

556 sulphur retention expected considering the reacted CaO during the experiments, i.e. 0.6%.
557 The real situation could be between those curves. Besides, the sulphur retention for the three
558 coals used in this work (lignite, bituminous Colombian coal and anthracite) was estimated in
559 Figure 11 (B). Obviously, the coal with lowest sulphur content achieved the highest sulphur
560 retentions. This was the case of the bituminous coal. In order to reach 54% sulphur retention
561 a lifetime of the particles of 100 h was required. Although the Tierga iron ore showed sulphur
562 retention capacity, too high makeup flows would be required and would make the process not
563 viable due to the short lifetime of the Tierga iron ore in the system.
564
565 In order to check if the high sulphur content in the combustion gases affected the Tierga iron
566 ore reactivity some experiments in a TGA using 15% H_2 at 950ºC were performed. Figure 12
567 shows the evolution of the reduction conversion with time. It has already been observed
568 before that the reactivity of the Tierga iron ore increased with the number of redox cycles
569 [24]. In Figure 12 the conversion curves for calcined and activated samples have been
570 included as reference. After 50 hours of hot fluidization during the experiments presented in
571 this work the Tierga iron ore increased its reactivity with time. The final value was close to
572 that of the activated sample. Therefore, no reactivity changes were detected.
573

574 ## 4. Conclusions

575
576 A highly reactive iron ore mainly based on hematite was tested as oxygen carrier in a 500W_{th}
577 continuous CLC unit as an alternative to other low-cost Fe-based materials proposed in
578 literature for the *i*G-CLC process. Experiments were performed using different coals, such as
579 lignite, bituminous Colombian coal and anthracite in the 875-930ºC interval.
580

581 The total oxygen demand using the Tierga iron ore was always below 4% for all the fuels.
582 Values lower than 2% were obtained with the bituminous coal or the lignite at the highest
583 temperature tested. As expected, the values of carbon capture efficiency increased for lower
584 rank coals reaching values around 45%, 57% and 94% for anthracite, bituminous coal and
585 lignite, respectively.
586
587 When compared to ilmenite and bauxite waste (Fe-ESF), lower values of oxygen demand
588 were obtained using the Tierga iron ore regardless of the temperature. No significant
589 differences in the carbon capture efficiencies and values higher than 95% will be expected for
590 ilmenite, Fe-ESF and Tierga iron ore if an efficient carbon separation unit between fuel and
591 air reactor is used.
592
593 An especial characteristic of this Tierga iron ore was the high CaO content (4.7%) that could
594 contribute to retain *in situ* the SO_2 generated in the fuel reactor during coal combustion. The
595 Tierga iron ore was capable of retaining the SO_2 generated but too high makeup flows would
596 be required in order to maintain the retention capacity.
597
598 No changes in the reactivity of the iron were observed after 50 hours of continuous hot
599 fluidization, the attrition rate was moderate (0.1%/h) and the mechanical strength was
600 maintained. Therefore this Tierga iron ore can be considered as an advantageous material to
601 be used in the further scale-up of the *i*G-CLC process.
602
603
604

Acknowledgments

The authors thank the Spanish Ministry for Science and Innovation (ENE2010-19550 project) and DGA-La Caixa (2012-GA-LC-076 project) for the financial support. This work was also partially supported by the European Commission, under the RFCS program (ACCLAIM Project, Contract RFCP-CT-2012-00006). T. Mendiara thanks for the "Juan de la Cierva" post-doctoral contract awarded by this Ministry. The authors also thank PROMINDSA for providing the solid material used in this work

613 **Bibliography**

614

615 [1] IEA International Energy Agency, CO_2 emissions from fuel combustion. Highlights 2010,
616 OECD/IEA, Paris, France.
617 [2] Adánez J, Abad A, García-Labiano F, Gayán P, de Diego LF. Progress in Chemical-
618 Looping Combustion and Reforming Technologies. A review. Prog Energ Combust 2012;38:
619 215-282.
620 [3] Dennis JS, Scott SA, Hayhurst AN. *In situ* gasification of coal using steam with chemical
621 looping: a technique for isolating CO_2 from burning a solid fuel. J Energy Inst 2006;79:187–
622 190.
623 [4] Leion H, Mattisson T, Lyngfelt A. The use of petroleum coke as fuel in chemical-looping
624 combustion. Fuel 2007;86:1947-1958.
625 [5] Cuadrat A, Abad A, de Diego LF, García-Labiano F, Gayán P, Adánez J. Prompt
626 considerations on the design of chemical-looping combustion of coal from experimental tests.
627 Fuel 2012;97:219-232.
628 [6] Cao Y, Pan WP. Investigation of chemical looping combustion by solid fuels. 1. Process
629 analysis. Energ Fuel 2006;20:1836-1844.
630 [7] Abad A, Gayán P, de Diego LF, García-Labiano F, Adánez J. Fuel reactor modelling in
631 chemical-looping combustion of coal: 1. model formulation. Chem Eng Sci 2013;87:277-293.
632 [8] Cuadrat A, Abad A, García-Labiano F, Gayán P, de Diego LF, Adánez J. Relevance of
633 the coal rank on the performance of the in situ gasification chemical-looping combustion.
634 Chem Eng J 2012;195-196:91-102.
635 [9] Cuadrat A, Abad A, García-Labiano F, Gayán P, de Diego LF, Adánez J. The use of
636 ilmenite as oxygen-carrier in a 500 W_{th} chemical-looping coal combustion unit. Int J Greenh
637 Gas Con 2011;5:1630-1642.

638 [10] Mendiara T, Abad A, de Diego LF, García-Labiano F, Gayán P, Adánez J. Biomass
639 combustion in a CLC system using an iron ore as oxygen carrier. Int J Greenh Gas Con.
640 2013;19:322-330.
641 [11] Mendiara T, Izquierdo MT, Abad A, de Diego LF, García-Labiano F, Gayán P, Adánez
642 J. Release of pollutant components in CLC of lignite. Int J Greenh Gas Con 2013; Accepted
643 for publication.
644 [12] Song T, Shen L, Xiao J, Chen D, Gu H, Zhang S. Nitrogen transfer of fuel-N in chemical
645 looping combustion. Combust Flame 2012;159:1286-1295.
646 [13] Shen L, Wu J, Xiao J, Song Q, Xiao R. Chemical-looping combustion of biomass in a 10
647 kW_{th} reactor with iron oxide as an oxygen carrier. Energ. Fuel 2009;23:2498-2505.
648 [14] Thon A, Kramp M, Hartge EU, Heinrich S, Werther J. Operational experience with a
649 coupled fluidized bed system for chemical looping combustion of solid fuels, in: Proc. 2nd Int.
650 Conf. Chemical Looping, Darmstadt, Germany, 2012.
651 [15] Sozinho T, Pelletant W, Staiton H, Guillou F, Gauthier T. Main results of the $10kW_{th}$
652 pilot plant operation, in: Proc. 2nd Int. Conf. Chemical Looping, Darmstadt, Germany, 2012.
653 [16] Linderholm C, Lyngfelt A, Cuadrat A, Jerndal E. Chemical-looping combustion of solid
654 fuels - Operation in a 10 kW unit with two fuels, above-bed and in-bed fuel feed and two
655 oxygen carriers, manganese ore and ilmenite, Fuel 2012;102:808-822.
656 [17] Markström P, Linderholm C, Lyngfelt A Chemical looping combustion of solid fuels –
657 design and operation of a 100 kW_{th} unit with bituminous coal. Int J Greenh Gas Con.
658 2013;15:150-162.
659 [18] Kempkes V, Kather A. Chemical Looping Combustion: comparative analysis of two
660 different overall process configurations for removing unburnt gaseous components, in: Proc.
661 2nd Int. Conf. Chemical Looping, Darmstadt, Germany, 2012.

662 [19] Gayán P, Abad A., de Diego LF, García-Labiano F, Adánez J. Assessment of
663 technological solutions for improving Chemical Looping Combustion of solid fuels with CO_2
664 capture. Chem Eng J 2013;233:56-69.
665 [20] García-Labiano F, de Diego LF, Gayán P, Abad A, Adánez J. Fuel reactor modelling in
666 chemical-looping combustion of coal: 2-simulation and optimization. Chem Eng. Sci
667 2013;87:173-182.
668 [21] Bayham SC, Kim HR, Wang D, Tong A, Zeng L, McGiveron O, Kathe MV, Chung E,
669 Wang W, Wang A, Majumder A, Fan LS. Iron-based coal direct chemical looping
670 combustion process: 200-h continuous operation of a 25-kW_{th} subpilot unit. Energ Fuel
671 2013;27:1347-1356.
672 [22] Mendiara T, de Diego LF, García-Labiano F, Gayán P, Abad A, Adánez J. Behaviour of
673 a bauxite waste material as oxygen carrier in a 500W_{th} CLC unit with coal. Int J Greenh Gas
674 Con 2013;17:170-182.
675 [23] Song T, Shen T, Shen L, Xiao J, Gu H, Zhang S. Evaluation of hematite oxygen carrier
676 in chemical-looping combustion of coal. Fuel 2013;104:244-252.
677 [24] Mendiara T, Pérez R, Abad A, de Diego LF, García-Labiano F, Gayán P, Adánez J.
678 Low-cost Fe-based oxygen carrier materials for the *i*G-CLC process with coal. 1. Ind Eng
679 Chem Res 2012;51:16216-16229.
680 [25] Abad A, Cuadrat A, Mendiara T, García-Labiano F, Gayán P, de Diego LF, Adánez J.
681 Low-cost Fe-based oxygen carrier materials for the *i*G-CLC process with coal. 2. Ind Eng
682 Chem Res 2012;51:16230-16241.
683 [26] Simell P, Stahlberg P, Kurkela E, Albretch J, Deutch S, Sjostrom K. Provisional protocol
684 for the sampling and analysis of tar and particulates in the gas from large-scale biomass
685 gasifiers. Version 1998. Biomass Bioenerg 2000;18:19-38.

686 [27] Mendiara T, Gayán P, Abad A, de Diego LF, García-Labiano F, Adánez J. Performance
687 of a bauxite waste as oxygen-carrier for chemical-looping combustion using coal as fuel. Fuel
688 Proc Technol 2013;109:57-69.
689 [28] Cuadrat A, Abad A, García-Labiano F, Gayán P, de Diego LF, Adánez J. Effect of
690 operating conditions in Chemical-Looping Combustion of coal in a 500 W_{th} unit. Int J Greenh
691 Gas Con 2012;6:153-163.
692 [29] Johnson JL. Fundamentals of Coal Gasification. Chapter 23, in: Elliot, M.A. (Eds.),
693 Chemistry of Coal Utilization. Wiley & Sons, New York; 1981.
694 [30] Cuadrat A, Abad A, Gayán P, de Diego LF, García-Labiano F, Adánez J. Theoretical
695 approach on the CLC performance with solid fuels: optimizing the solids inventory. Fuel
696 2012;97:536-551.
697 [31] Abad A, Adánez J, de Diego LF, Gayán P, García-Labiano F, Lyngfelt A. Fuel reactor
698 model validation: assessment of the key parameters affecting the chemical-looping
699 combustion of coal. Int J Greenh Gas Con 2012;19:541-551.
700
701
702
703
704
705
706

Nomenclature

C_{fixed}: percentage of fixed carbon (%)

C_{coal}: carbon percentage in coal (%)

$F_{CO_2,AR}$: carbon dioxide molar flow in the air reactor (mol/s)

$F_{i,FR}$: i species molar flow in the fuel reactor inlet/outlet stream (mol/s)

$F_{C,vol}$: carbon flow from the volatile matter (mol/s)

K_i: constant considering the inhibitory effect in equation (16)

k_{react}: kinetic constant in equation (16)

M_O: molar mass of oxygen (0.016 kg/mol)

M_{O_2} : molar mass of molecular oxygen (0.032 kg/mol)

$\dot{m}_{OC}$: solid circulation rate (kg/s)

$\dot{m}_{SF}$: coal feeding rate (kg/s)

$m_{OC,FR}$: mass of oxygen carrier in the fuel reactor (kg)

$m_{s,FR}$: mass inventory in the fuel reactor (kg oxygen carrier/MW_{th})

p_{prod}: partial pressure of the gasification products (CO and H_2) (bar)

p_{react}: partial pressure of the gaseous reactants (bar)

$(-r_C)$: instantaneous rate of char conversion (s^{-1})

$(-r_O)$: rate of oxygen transferred from the oxygen carrier to the fuel (mol/s)

R_{OC}: oxygen transport capacity

t_{res}: residence time in the fuel reactor (s)

X_{char}: char conversion

Greek symbols

ϕ : oxygen carrier to fuel ratio

Ω_{SF}: coal oxygen demand (kg oxygen/kg coal)

Ω_T: total oxygen demand

732 η_{CC}: carbon capture efficiency

733 η_{CC}^{*}: carbon capture efficiency considering elutriation

734 η_{CSS}: carbon separation efficiency in the carbon separation unit

735 **List of Figure Captions**

736 **Figure 1.** Experimental unit ICB-CSIC-s1

737 **Figure 2.** (A) Oxygen demand and (B) carbon capture efficiency (Closed symbols (η_{CC}) and
738 open symbols (η_{CC}^{*})) dependence on temperature in experiments with lignite (L), bituminous
739 Colombian coal (HVB) and anthracite (A) at different T_{FR} using Tierga iron ore as oxygen
740 carrier. Conditions: $\phi = 1$; L = 2023 kg/MW_{th}; HVB = 1463 kg/MW_{th}; A = 2847 kg/MW_{th};

741 **Figure 3.** (A)Total oxygen demand and (B) rate of oxygen transferred dependence on
742 temperature in experiments with a bituminous Colombian coal (HVB) at different T_{FR} using
743 ilmenite, Fe-ESF material (data in [22], oxygen demand recalculated) and Tierga iron ore
744 (Fe-ore). Conditions: $\phi = 1$; Ilmenite: 3140 kg/MW_{th}; Fe-ESF: 2850 kg/MW_{th}; Tierga iron
745 ore: 1463 kg/MW_{th}

746 **Figure 4.** (A) Carbon capture efficiency and (B) char gasification rate dependence on
747 temperature in experiments with a bituminous Colombian coal (HVB) at different T_{FR} using
748 ilmenite, Fe-ESF material [22] and Tierga iron ore (Fe-ore). Conditions: $\phi = 1$; Ilmenite:
749 3140 kg/MW_{th}; Fe-ESF: 2850 kg/MW_{th}; Tierga iron ore: 1463 kg/MW_{th}

750 **Figure 5.** Comparison of experimental and theoretical values for the char gasification rate of
751 the bituminous Colombian coal (HVB) in the experiments with ilmenite, the Fe-ESF material
752 and Tierga iron ore at 920ºC as function of the $CO+H_2$ concentration at the outlet of the fuel
753 reactor. Conditions: $\phi = 1$; Ilmenite: 3140 kg/MW_{th}; Fe-ESF: 2850 kg/MW_{th}; Tierga iron ore:
754 1463 kg/MW_{th}

755 **Figure 6.** Estimated values of the carbon capture efficiency at 920ºC with a bituminous
756 Colombian coal (HVB) for different values of the efficiency in the carbon separation unit
757 (η_{CSS}). Conditions: $\phi = 1$; Ilmenite: 3140 kg/MW_{th}; Fe-ESF: 2850 kg/MW_{th}; Tierga iron ore:
758 1463 kg/MW_{th}

Figure 7. Evolution with time of the attrition rate in the experiments using Tierga iron ore and different coals as fuel: anthracite (A), bituminous Colombian coal (HVB) and lignite (L).

Figure 8. Evolution with time of the SO_2 concentration in the fuel reactor in experiments with lignite and Tierga iron ore at 915ºC. A, B and C indicate the measurements which were accompanied by sample taking: A = 0.5 h; B = 2 h; C = 5 h.

Figure 9. SEM images of the Tierga iron ore particles after calcination and after used in the continuous unit during 50 hours of hot fluidization

Figure 10. Sulphur splitting in experiments with ilmenite and Tierga iron ore: $\mathbf{FR_g}$ (fuel reactor gas outlet) $\mathbf{AR_g}$ (air reactor gas outlet) **Pyr** (pyritic sulphur in ashes) **Ash** (self-retention by ashes)

Figure 11. Sulphur retention (%) for different lifetimes of the Tierga iron ore (1 MW_{th}) (A) using ilmenite as fuel (B) using different fuels and CaO = 4.7%

Figure 12. Conversion for the Tierga iron ore during reduction versus time after 50 hours of hot fluidization in the continuous unit. Conditions: 15 % H_2 at T = 950ºC

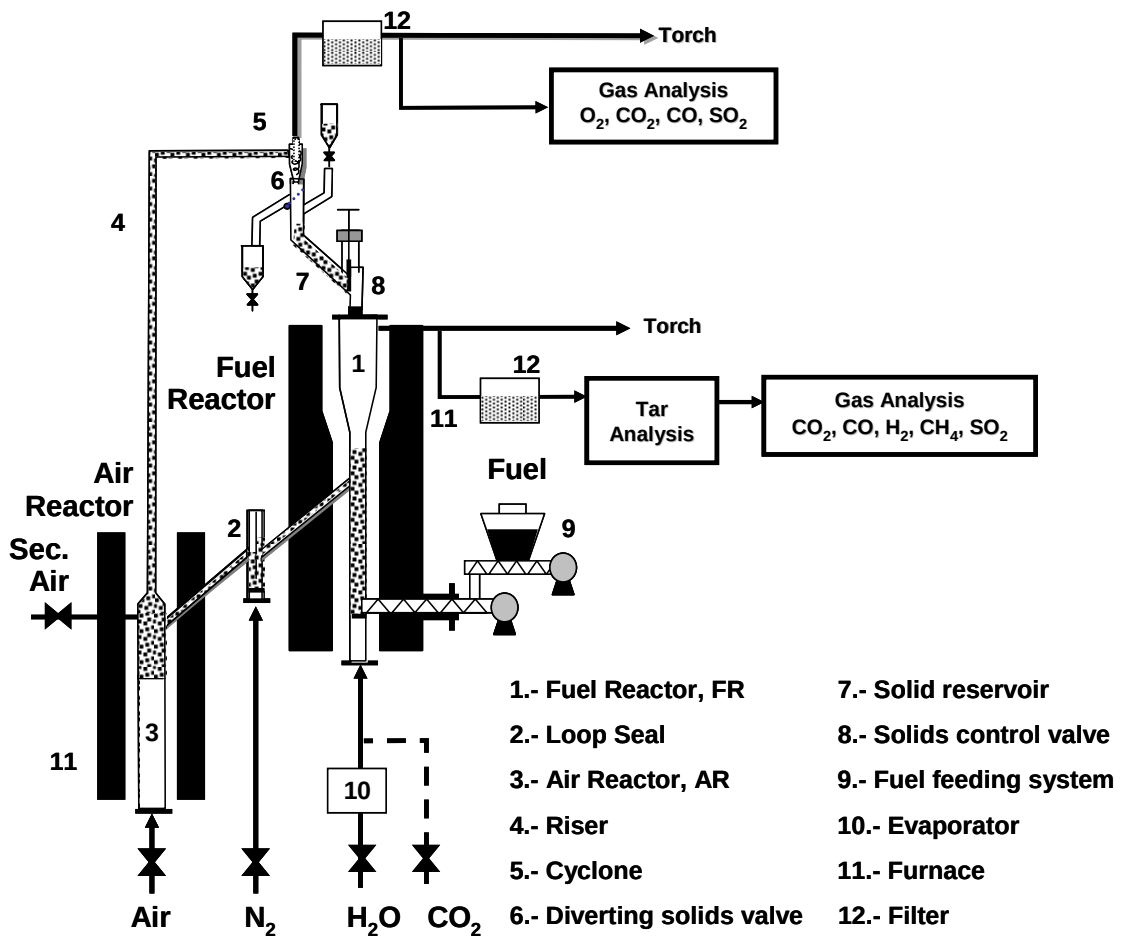

Figure 1. Experimental unit ICB-CSIC-s1

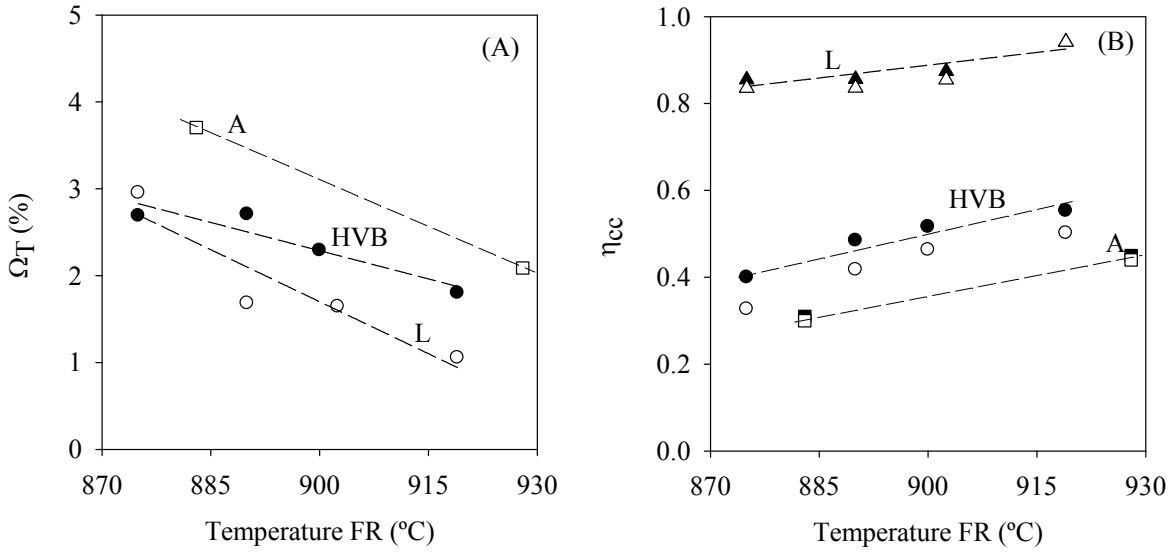

802

803 **Figure 2.** (A) Oxygen demand and (B) carbon capture efficiency (Closed symbols (η_{CC}) and
804 open symbols (η_{CC}^{*})) dependence on temperature in experiments with lignite (L), bituminous
805 Colombian coal (HVB) and anthracite (A) at different T_{FR} using Tierga iron ore as oxygen
806 carrier. Conditions: $\phi = 1$; L = 2023 kg/MW_{th}; HVB = 1463 kg/MW_{th}; A = 2847 kg/MW_{th};

807

808

809

810

811

812

813

814

815

816

817

818

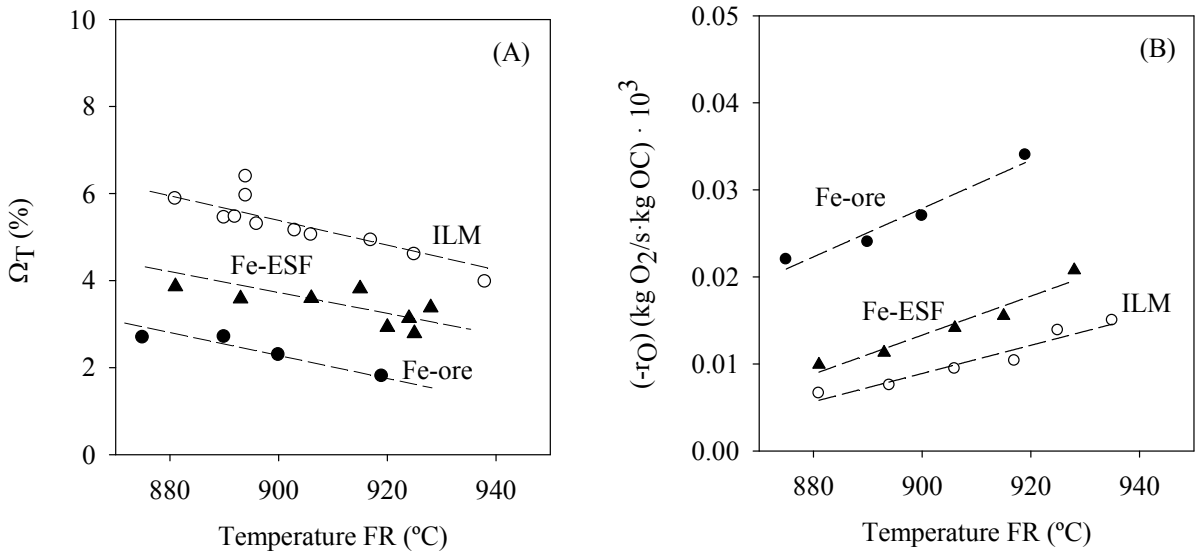

819

820 **Figure 3.** (A)Total oxygen demand and (B) rate of oxygen transferred dependence on
821 temperature in experiments with a bituminous Colombian coal (HVB) at different T_{FR} using
822 ilmenite, Fe-ESF material (data in [22], oxygen demand recalculated) and Tierga iron ore
823 (Fe-ore). Conditions: $\phi = 1$; Ilmenite: 3140 kg/MW_{th}; Fe-ESF: 2850 kg/MW_{th}; Tierga iron
824 ore: 1463 kg/MW_{th}

825

826

827

828

829

830

831

832

833

834

835

836

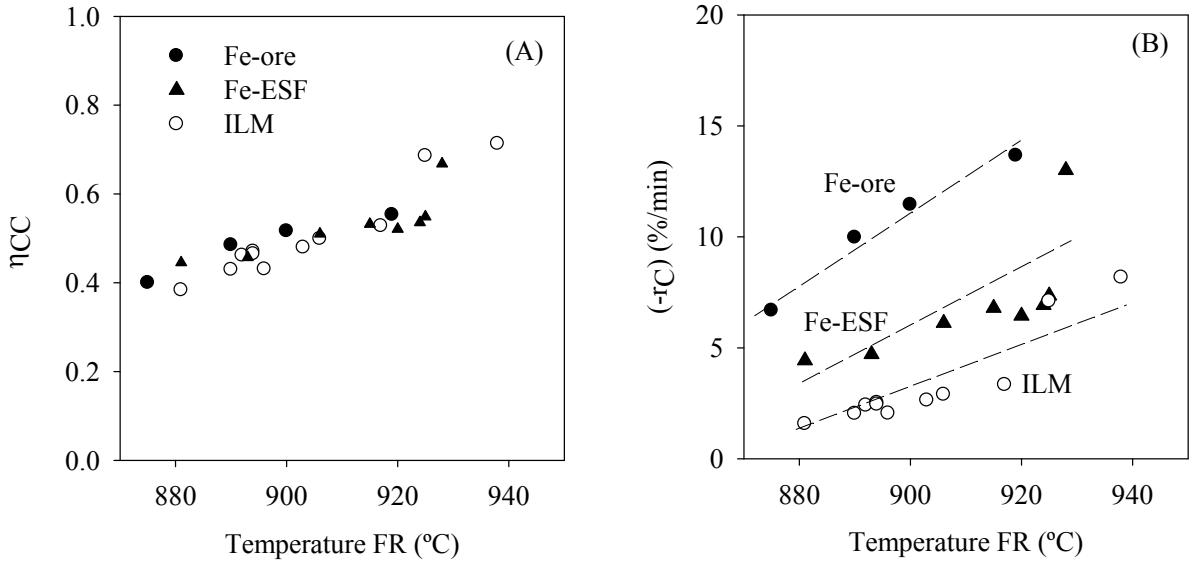

837

838 **Figure 4.** (A) Carbon capture efficiency and (B) char gasification rate dependence on
839 temperature in experiments with a bituminous Colombian coal (HVB) at different T_{FR} using
840 ilmenite, Fe-ESF material [22] and Tierga iron ore (Fe-ore). Conditions: $\phi = 1$; Ilmenite:
841 3140 kg/MW_{th}; Fe-ESF: 2850 kg/MW_{th}; Tierga iron ore: 1463 kg/MW_{th}

842

843

844

845

846

847

848

849

850

851

852

853

854

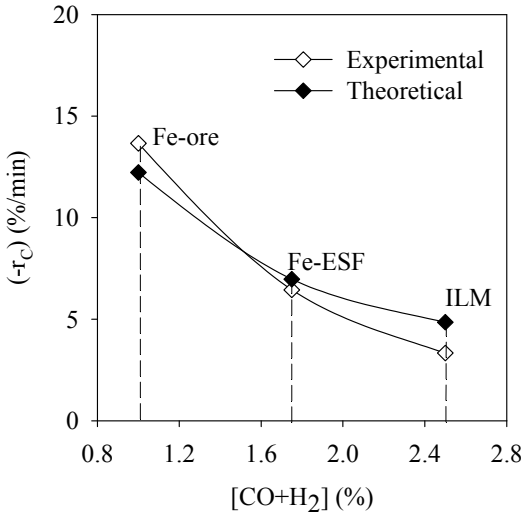

855

856 **Figure 5.** Comparison of experimental and theoretical values for the char gasification rate of
857 the bituminous Colombian coal (HVB) in the experiments with ilmenite, the Fe-ESF material
858 and Tierga iron ore at 920ºC as function of the $CO+H_2$ concentration at the outlet of the fuel
859 reactor. Conditions: $\phi = 1$; Ilmenite: 3140 kg/MW_{th}; Fe-ESF: 2850 kg/MW_{th}; Tierga iron ore:
860 1463 kg/MW_{th}

861

862

863

864

865

866

867

868

869

870

871

872

873

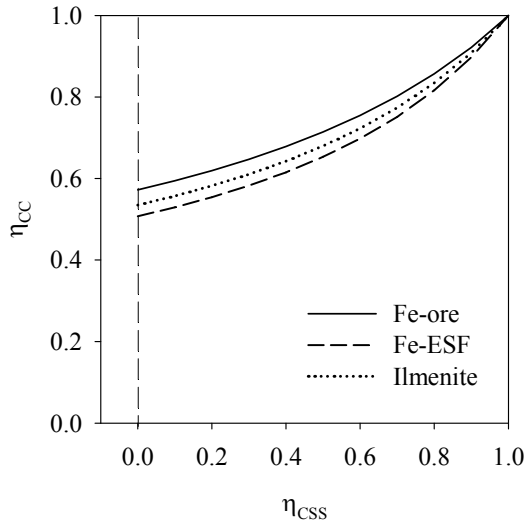

874

875 **Figure 6.** Estimated values of the carbon capture efficiency at 920ºC with a bituminous
876 Colombian coal (HVB) for different values of the efficiency in the carbon separation unit
877 (η_{CSS}). Conditions: $\phi = 1$; Ilmenite: 3140 kg/MW_{th}; Fe-ESF: 2850 kg/MW_{th}; Tierga iron ore:
878 1463 kg/MW_{th}

879

880

881

882

883

884

885

886

887

888

889

890

891

892

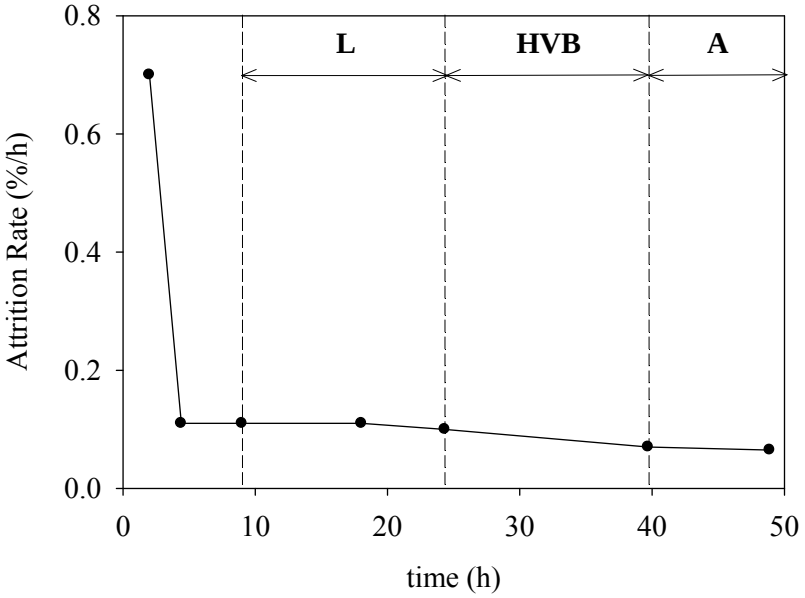

893

894 **Figure 7.** Evolution with time of the attrition rate in the experiments using Tierga iron ore

895 and different coals as fuel: anthracite (A), bituminous Colombian coal (HVB) and lignite (L).

896

897

898

899

900

901

902

903

904

905

906

907

908

909

910

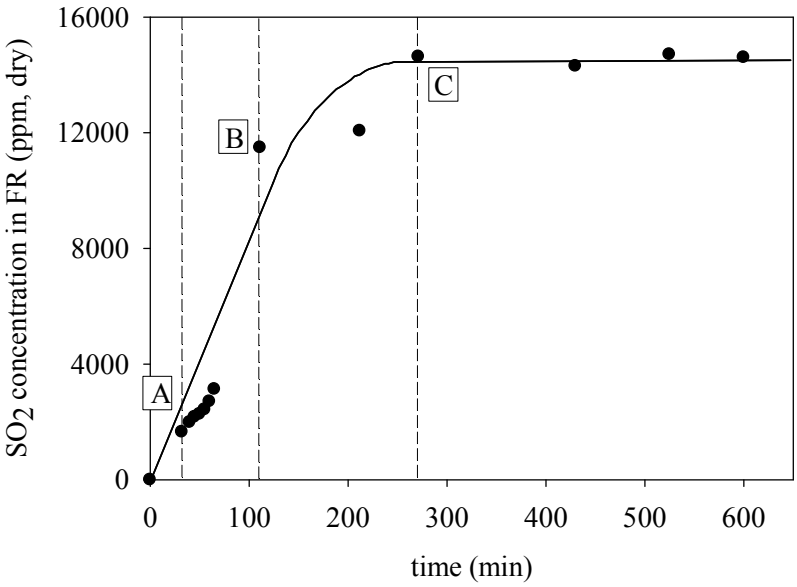

911

912 **Figure 8.** Evolution with time of the SO_2 concentration in the fuel reactor in experiments
913 with lignite and Tierga iron ore at 915ºC. A, B and C indicate the measurements which were
914 accompanied by sample taking: A = 0.5 h; B = 2 h; C = 5 h.

915

916

917

918

919

920

921

922

923

924

925

926

927

928

929

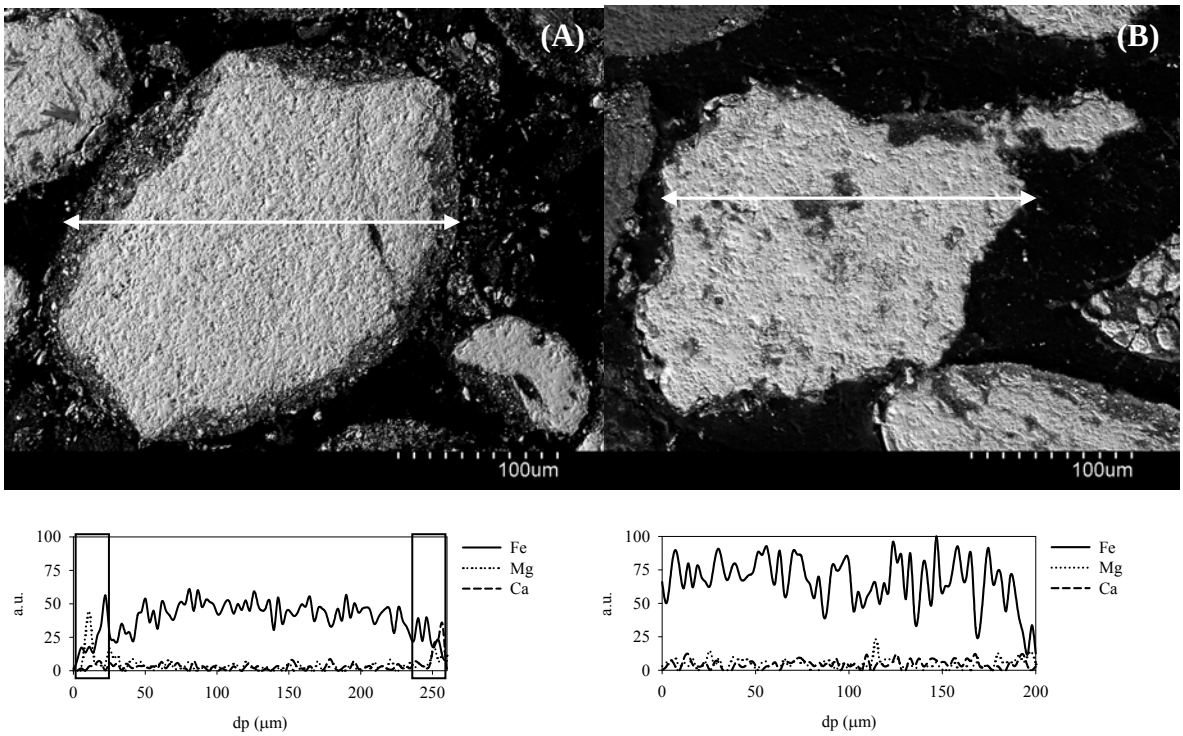

930

931 **Figure 9.** SEM images of the Tierga iron ore particles after calcination and after used in the

932 continuous unit during 50 hours of hot fluidization

933

934

935

936

937

938

939

940

941

942

943

944

945

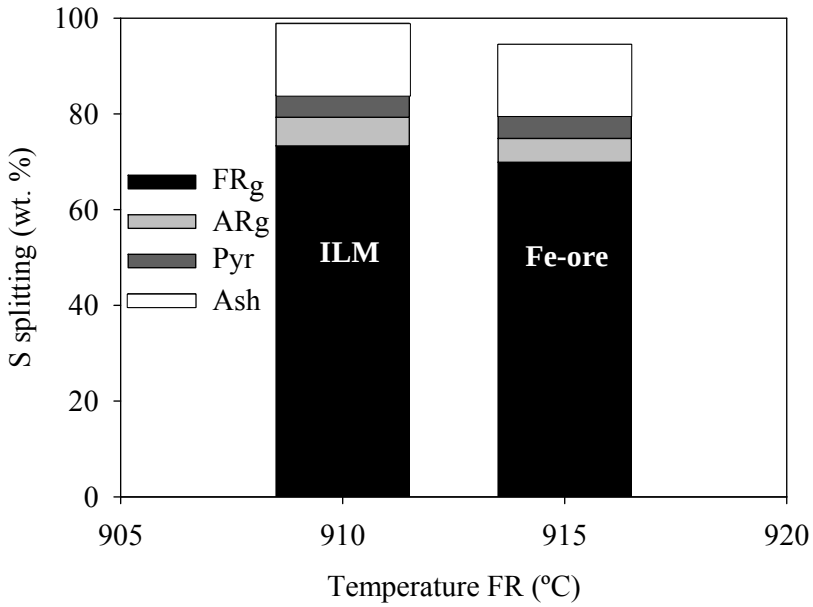

946

947 **Figure 10.** Sulphur splitting in experiments with ilmenite and Tierga iron ore: **FR_g** (fuel
948 reactor gas outlet) **AR_g** (air reactor gas outlet) **Pyr** (pyritic sulphur in ashes) **Ash** (self-
949 retention by ashes)

950

951

952

953

954

955

956

957

958

959

960

961

962

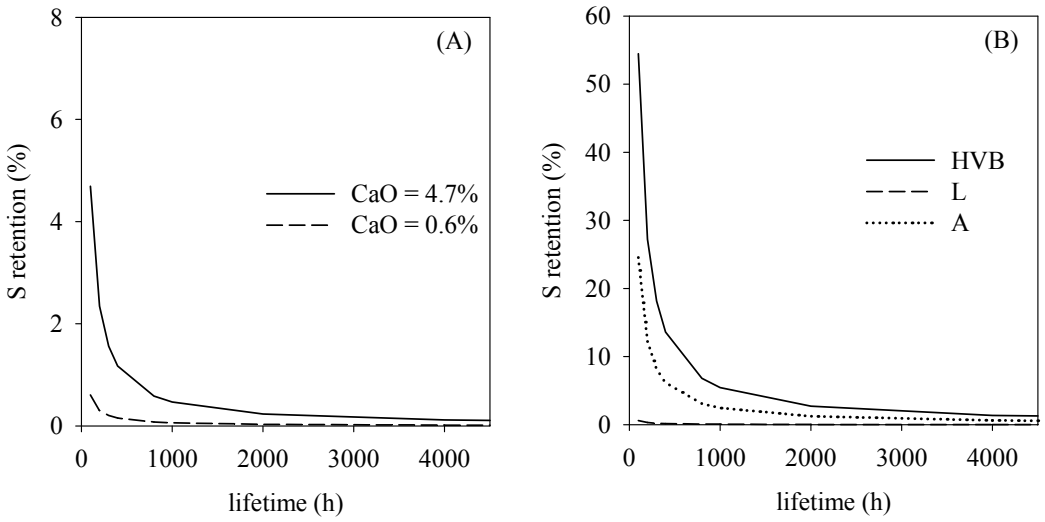

963

964 **Figure 11.** Sulphur retention (%) for different lifetimes of the Tierga iron ore (1 MW_{th}) (A)

965 using ilmenite as fuel (B) using different fuels and CaO = 4.7%

966

967

968

969

970

971

972

973

974

975

976

977

978

979

980

981

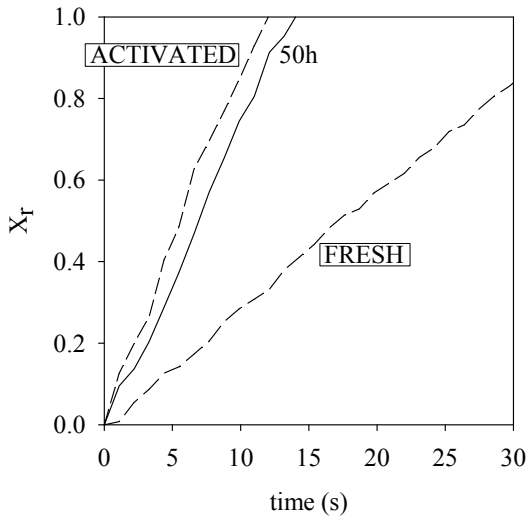

Figure 12. Conversion for the Tierga iron ore during reduction versus time after 50 hours of hot fluidization in the continuous unit. Conditions: 15 % H_2 at T = 950ºC

Tables

Table 1. Characterization of the iron ore after calcination

Fe_2O_3 (% wt)	76.5[a]
XRD main phases	Fe_2O_3, SiO_2, Al_2O_3, CaO, MgO,
Crushing strength (N)	5.8
Oxygen transport capacity, R_{OC}, (%)[b]	2.5
Porosity (%)	26.3
Skeletal density (kg/m^3)	4216
Specific surface area, BET (m^2/g)	1.4

[a] Determined by TGA

[b] $R_{OC} = \frac{m_o - m_r}{m_o}$

Table 2. Ultimate and proximate analyses of the coals used as fuels (as received)

	Anthracite	**Bituminous**	**Lignite**
Proximate analysis			
Moisture	1.0	2.3	12.5
Ash	31.5	8.8	25.2
Volatile matter	7.5	33.0	28.6
Fixed carbon	59.9	55.9	33.6
Ultimate analysis			
Carbon	60.7	65.8	45.4
Hydrogen	2.0	3.3	2.5
Nitrogen	0.9	1.6	0.6
Sulfur	1.3	0.6	5.2
Oxygen[a]	2.7	17.9	9.9
LHV (kJ/kg)	21878	21900	16251

[a] By difference

Table 3. Composition of the iron ore determined by ICP

Compound	**% wt**
Al_2O_3	4.0
CaO	4.7
Fe_2O_3	78.8
K_2O	1.1
MgO	3.0
Na_2O	0.1
SiO_2	8.2
TiO_2	0.1